Original Article
Food Science and Technology

ISSN 0101-2061 (Print)
ISSN 1678-457X (Online)

DOI: https://doi.org/10.1590/fst.67820

Enzymatic hydrolysis of a colloidal system based on cape gooseberry

Soany ERASO-GRISALES[1]*, Misael CORTES-RODRÍGUEZ[1], Hader Iván CASTAÑO-PELÁEZ[2], Andrés HURTADO-BENAVIDES[3]

Abstract

The objective of this research was to evaluate the influence of the enzymatic process on the physicochemical stability of a colloidal system based on cape gooseberry pulp, skin, and seeds (CS_{CG}). The pulp, seed, and skin mixture were homogenized by shearing in a rotor-stator system at 10,000 rpm. A completely randomized factorial design was used, considering the independent variables: Viscozyme® L enzyme concentration [Enzyme] (50, 125, and 200 ppm) and hydrolysis time (HT) (0, 30, 60, 90, and 120 minutes), and the dependent variables: viscosity (μ), zeta potential (ζ), particle size (percentiles D_{10}, D_{50}, and D_{90}), spectral absorption index (R). Both independent variables had a significant impact on the process. [Enzyme] affected mainly μ, D_{50}, D_{90}, and R and HT affected μ and D_{10}. The optimization of the formulation was performed under the criterion of obtaining a CS_{CG} with higher physicochemical stability. The optimization showed desirability of 74.2% with [Enzyme] at 78.5 ppm and HT of 120 minutes. The dependent variables obtained experimentally were: μ = 371.3 ± 24.2 cP, ζ = -21.8 ± 0.3 mV, D_{10} = 3.5 ± 0.3 μm, D_{50} = 135 ± 3.6 μm, D_{90} = 565.7 ± 25.5 μm, and R = 0.655 ± 0.007. The integration of homogenization processes and enzymatic treatments contributed to obtaining a physicochemical stable colloidal system based on cape gooseberry pulp, skin, and seeds.

Keywords: *Physalis peruviana* L.; colloidal stability; enzymatic treatments; agro-industrial wastes; homogenization.

Practical application: *Enzymatic hydrolysis and physicochemical stability of a colloidal cape gooseberry*

1 Introduction

The cape gooseberry is a juicy berry of the *Physalis peruviana* L. plant, its shape is spherical or ovular that contains seeds inside, and its skin is thin and waxy. The cape gooseberry pulp represents approximately 73.6% of the total weight of the fruit; while the seeds and skin are 27.4% (Ramadan & Morsel, 2003), the latter is little used in production systems (Ramadan et al., 2008). The fruit is consumed naturally in salads, jams, and juices and is an excellent source of vitamin A and C. It also has significant amounts of B complex vitamins (thiamine, niacin, and vitamin B_{12}) and high protein and phosphorus levels (Olivares et al., 2016). On the other hand, it contains antioxidant compounds such as tocopherols and carotenoids. Also have other compounds such as withanolides have repellent, immunomodulatory, antibacterial, anti-inflammatory, antitumor, and antihepatotoxic activity (Puente et al., 2011; Ramadan, 2011a). The seeds are an essential source of essential fatty acids that contain natural antioxidants and high levels of phytosterols, which have cholesterol-lowering effects. Notably, campesterol, β-sitosterol, and stigmasterol can be responsible for the decrease in cholesterol levels in the blood and LDL-cholesterol concentrations in plasma by inhibiting cholesterol absorption in the intestine in a competitive process structural similarity between plant sterols and cholesterol (Nocetti et al., 2020).

Additionally, the skin and pulp contain important pectins, such as the primary dietary fiber (4.9 g/100 g) (Ramadan, 2011b). In general, these characteristics make the cape gooseberry desired worldwide by the modern consumer, providing multiple health benefits; it has besides been used as a natural medicine to prevent degenerative diseases, as it has anti-cancer properties (Mokhtar et al., 2018; Puente et al., 2011; Ramadan, 2011a). It prevents metabolic alterations associated with obesity in the liver and skeletal muscle (Fuente et al., 2020) besides exerts cytoprotective and antioxidant effects on brain cells exposed to neurotoxic stimuli (Areiza-Mazo et al., 2018).

Fruit juices are complex and heterogeneous colloidal insoluble particles dispersed in a continuous medium rich in soluble compounds, including sugars, organic acids, soluble pectins, phenolic compounds, and salts. The dispersed material is formed mainly by fragments of cellular tissues derived in its composition (Dahdouh et al., 2016). Colloidal systems are thermodynamically unstable, governed by Brownian motion; they depend on various physicochemical components: surface, electrostatic, adsorption, molecular, and interparticle interactions, as well as hydrocolloid properties (Wan et al., 2019). Among the forces responsible for the physicochemical stability of the colloidal system, the attractive or Van der Waals forces and the repulsive or electrostatic forces stand out; in addition, there

Received 14 Dec., 2020
Accepted 18 Aug., 2021
[1] *Facultad de Ciencias Agrarias, Universidad Nacional de Colombia, Medellín, Antioquia, Colombia*
[2] *Facultad de Ciencias Básicas, Sociales y Humanas, Politécnico Colombiano Jaime Isaza Cadavid, Medellín, Antioquia, Colombia*
[3] *Facultad de Ingeniería Agroindustrial, Universidad de Nariño, Pasto, Nariño, Colombia*
*Corresponding author: skerasog@unal.edu.co

are others such as steric, hydration, hydrophobic, and phase separation forces (Hennart et al., 2010). The use of shear or other homogenization processes and the modification of the rheology of the continuous phase contribute to the stability of the colloidal system by decreasing the attractive forces (< particle size) and the mobility of the particles (Chen et al., 2014; Hua et al., 2017; Ozyurt & Ötles, 2016). Dahdouh et al. (2016) reported that the physicochemical interactions between the particles are closely related to the biochemical composition of the fruit juice, particularly by the presence of polysaccharides, such as pectins, cellulose, and hemicellulose. In this sense, the insoluble particles present (pectin, cellulose, hemicellulose, lignin, among others) are responsible for turbidity and phase separation (sedimentation). The development of this turbidity results from the previous formation of polymeric complexes between polysaccharides, low molecular weight solutes (sugars and metal ions), and proteins (Uzuner & Cekmecelioglu, 2018). In this sense, various parameters and methods have been used to evaluate the stability of colloidal systems: spectral absorption index (R), zeta potential (ζ), viscosity (μ), distribution and size of particles, total solids (TS), surface tension, among others (Matusiak & Grządka, 2017).

Hydrolytic enzymes and enzyme complexes (amylases, pectinases, cellulases, and hemicelluloses) have been used in the beverage industry to the improvement of the final properties of the product: yield, clarification, and reduction of sediments, extraction of bioactive components from fruits (Álvarez, 2018; Ramadan, 2018; Singh et al., 2019; Uzuner & Cekmecelioglu, 2018). In this context, pectinase enzyme has been used in litchi juice concentrate (100-500 ppm, 40 °C, and 2 h), at 500 ppm facilitated the reduction of insoluble solids and produced lychee juice whit less viscosity (Vijayanand, Kulkarni, & Prathibha, 2010). Pectinex SP-L® (pectinases, hemicellulases, and beta-glucanases) and Rapidase TF® (pectinase, cellulase, and hemicellulase) (100-300 ppm, 35-55 °C, 2 h) have been used in umbu pulp, where 100 ppm of Rapidase - 35 °C - 40 min, enabled the viscosity reduction and greater preserving the vitamin C (Gouvêa et al., 2017). Pectinex SP-L® with α-amylase and Pectinex SP-L® with cellulase (1.5-0.5% v/w, 50 °C - 2 h) has been used in soursop puree, where Pectinex SP-L® with cellulase reduced the viscosity up to 50%, and puree produced had a lower pH, and more content of total sugar and organic acid (Chang et al., 2018). In cape gooseberry pulp, Ramadan & Moersel (2007) evaluated the influence of enzyme complexes (pectinase, protease and hemicellulase, polygalacturonase and cellulase) at 250 ppm, 50 °C for 2 h. The authors report that the treatments increased the juice yield and the macro and micro component contents. Besides, juices with higher pulp content, higher acidity, and a higher quantity of total soluble solids (SS) are produced.

In this context, the objective of this research was to evaluate the influence of the enzymatic process on the physicochemical stability of a colloidal system based on pulp, skin, and cape gooseberry seed (CS_{CG}); allowing the full use of the cape gooseberry matrix (sustainable process) and more excellent added value.

2 Materials and methods

2.1 Materials

Colombian Ecotype cape gooseberries from the eastern municipalities of Antioquia, Colombia, were selected with degrees of maturity 3 and 4, according to the Colombian Technical Standard NTC 4580 (Instituto Colombiano de Normas Técnicas y Certificación, 1999). The fruits were disinfected by immersion in a 1400 ppm solution of Citrosan® (0.25% v/v) (Diken International, Mexico) for 10 minutes; then, the mixture of pulp, skin, and seed, was homogenized in a rotor and stator type equipment (Silverson Machines Ltd, England, model L5M) for 10 minutes at 10,000 rpm until obtaining the CS_{CG}.

On the other hand, Viscozyme® L (Novozymes, Denmark), a multi-enzyme complex from a strain of the fungus *Aspergillus aculeatus*, was used because it contains a wide range of carbohydrases (arabanase, cellulase, β-glucanase, hemicellulose, and xylanase) with an activity of ≥100 fungal β-glucanase units/g. The Enzyme also has activity against the branched pectin-like substances found in fruits and vegetables (Vong & Liu, 2019).

2.2 Enzymatic process

Batches of 4000 g of homogenized CS_{CG} were processed by enzymatic hydrolysis using Viscozyme® L (Novozymes, Denmark). Initially, the homogenized pulp was subjected to a sonication process (Branson 3510 Ultrasonic Cleaner, USA) for 15 minutes, 40 Hz, and controlled temperature (≈30 °C). Subsequently, the Enzyme was added, and the mixture was incubated in a thermostated bath (Memmert WNB, Germany) (30 ± 0.5 °C) under slow stirring (Sammic TR-350) during the HT. A control sample was additionally prepared without the use of enzymes, and the enzymatic hydrolysis was evaluated, taking a 200 mL aliquot every 30 minutes, and enzyme inactivation was performed at the end of each treatment, heating the CS_{CG} at 90 ° C for 5 minutes. (Ramadan & Moersel, 2007). The enzymatic process applied to CS_{CG} was evaluated through a completely randomized factorial design (15 experiments), considering the independent variables: enzyme concentration [Enzyme] (50, 125, and 200 ppm) and hydrolysis time (HT) (0, 30, 60, 90, and 120 min), and the dependent variables: μ, ζ, particle size (D_{10}, D_{50}, D_{90}) and R.

2.3 Characterization methods

- **pH** was determined according to the standard AOAC 981.12 (Association of Official Analytical Chemists, 2012) with a potentiometer (Hanna, USA, model pH 211) after calibrating the equipment with pH buffer solutions = 4 and pH = 7 at 25 °C.
- μ was determined in a rheometer (Brookfield DV-III Ultra, Brookfield Engineering Laboratories, Inc, USA) coupled to a temperature-controlled bath (25 °C) (Brookfield, model TC-502, USA) with an RV3 spindle. The test was carried out with deformation speeds from 0.01 to 100 rpm, and the value was reported at 100 rpm (Wardy et al., 2014).

- ζ was determined according to the methodologies described by Wellala et al. (2020), with some modifications. For this, a Zetasizer Nano ZS90 equipment (Malvern Instruments Ltd., Worcester, UK) was used, the suspension was diluted in deionized water (1: 100) and injected into a 1 mL capillary electrophoresis cell.
- **Particle sizes (D_{10}, D_{50}, and D_{90} percentiles)** were determined by laser light diffraction in a Mastersizer 3000 Hydro LV system (Malvern Instrument Ltd, Worcestershire, UK), according to the methodology of Dahdouh et al. (2018), where the CS_{CG} refractive index was set to 1.368, the water refractive index at 1.33, the particle absorption index (0.45), and the level of laser obscuration at 15.
- **R** was determined in a UV-Visible spectrophotometer (Thermo Scientific Evolution 60, USA), according to the methodology described by Gallón et al. (2020). It was defined as the absorbance ratio at 800 nm over 400 nm (A800/A400); the sample was diluted in deionized water (1:100). As a blank, was used deionized water

2.4 Statistical Analysis

The results were analyzed with the Statgraphics Centurion XVII.II software, through an analysis of variance (ANOVA) at a significance level of 5% ($p < 0.05$). The experimental process optimization was carried out according to defined and desirable criteria in the CS_{CG}; while, the impacts and weights were defined based on the results of the ANOVA. The results of the dependent variables were adjusted to a second-order polynomial model (Equation 1), where Y is the dependent variable, β_0 is constant, β_A and β_B are the linear coefficients; $\beta_A{}^2$ and $\beta_B{}^2$ are the quadratic coefficients, and β_{AB} is the coefficient of the linear interaction of the factors.

$$Y = \beta_0 + \beta_A A + \beta_B B + \beta_A{}^2 A^2 + \beta_B{}^2 B^2 + \beta_{AB} AB \quad (1)$$

3 Results and discussion

3.1 Design of the colloidal system based on cape gooseberry pulp, skin, and seeds

The mean pH values CS_{CG} were within the range (3.6 - 3.7); these values are within the optimal pH range of the Viscozyme® L enzyme complex (3.3-5.5) (Kitrytė et al., 2017).

Table 1 and 2 present the mean values ± standard deviation and the ANOVA results as a function of the p-value of CS_{CG} dependent variables treated by enzymatic hydrolysis, respectively. On the other hand, Figure 1 presents the response surface graphs.

The μ presented statistically significant differences ($p < 0.05$) with respect to the dependent variables [Enzyme], HT, the linear interaction [Enzyme]-HT, and the quadratic interaction of [Enzyme], because of fluctuations in their mean values (620.0-240.5 cP). The μ of CS_{CG} is a function of the intermolecular forces and the water-solute interactions, and these forces depend on the intermolecular spaces and the forces of the H_2 bond (López-Esparza et al., 2015). It is observed that the μ of CS_{CG} at the beginning of the enzymatic processes presented the lowest values, conferring a modification in enzymatic activity based on HT and being higher at high [Enzyme].

This could be attributed to the fact that the multi-active enzyme complex Viscozyme® L effectively hydrolyzes polysaccharides in plant cells, breaks the bonds within the polysaccharide matrix, and facilitates the release of more intercellular components, such as proteins, fatty acids (linoleic, oleic, palmitic, and stearic), and phytosterols, among others (Agarwal & Bosco, 2014; Puente et al., 2011; Ramadan & Morsel, 2003).

This action is enhanced by the prior homogenization by shearing that defragments the structure, increasing the enzyme action due to the increase in the surface area of the particles, mainly seeds, and skin. When added to the water-soluble

Table 1. Results of the dependent variables of CS_{CG}.

Treatment	[Enzyme] (ppm)	HT (min)	μ (cP)	ζ (mV)	Particle size			R
					D_{10} (μm)	D_{50} (μm)	D_{90} (μm)	
1	50	0	357.0 ± 1.0	-17.0 ± 0.9	11.1 ± 0.4	136.3 ± 7.4	477.3 ± 53.8	0.635 ± 0.004
2	125	0	269.0 ± 2.0	-17.7 ± 0.5	11.2 ± 0.1	129.0 ± 7.0	515.0 ± 46.9	0.669 ± 0.005
3	200	0	356.5 ± 8.5	-17.6 ± 0.8	12.7 ± 0.6	156.0 ± 3.6	600.3 ± 21.1	0.702 ± 0.002
4	50	30	373.0 ± 20.0	-18.2 ± 0.4	6.5 ± 0.2	109.0 ± 5.6	454.3 ± 36.7	0.631 ± 0.003
5	125	30	240.5 ± 6.5	-20.8 ± 0.5	4.3 ± 0.5	129.1 ± 22.8	590.9 ± 87.0	0.540 ± 0.007
6	200	30	518.5 ± 7.5	-17.5 ± 0.3	5.5 ± 0.2	137.7 ± 5.5	559.7 ± 10.5	0.743 ± 0.010
7	50	60	383.0 ± 23.0	-18.9 ± 0.9	5.4 ± 0.2	104.1 ± 4.1	459.0 ± 10.0	0.636 ± 0.003
8	125	60	308.0 ± 8.0	-20.1 ± 0.9	3.1 ± 0.1	116.5 ± 15.5	511.3 ± 41.0	0.585 ± 0.018
9	200	60	521.0 ± 10.0	-17.4 ± 0.3	4.0 ± 0.3	142.3 ± 11.6	649.3 ± 31.8	0.773 ± 0.005
10	50	90	414.5 ± 7.5	-17.3 ± 0.9	4.0 ± 0.1	107.6 ± 6.7	465.7 ± 31.0	0.671 ± 0.002
11	125	90	308.5 ± 8.5	-17.3 ± 0.9	2.4 ± 0.2	105.0 ± 15.2	449.3 ± 48.8	0.559 ± 0.027
12	200	90	582.0 ± 13.0	-16.2 ± 0.6	3.5 ± 0.1	135.0 ± 10.6	586.0 ± 31.3	0.784 ± 0.012
13	50	120	416.0 ± 8.0	-17.0 ± 0.4	3.2 ± 0.1	115.7 ± 7.1	495.0 ± 22.9	0.668 ± 0.004
14	125	120	374.0 ± 24.0	-20.8 ± 0.7	2.4 ± 0.1	130.3 ± 17.6	502.0 ± 26.5	0.574 ± 0.007
15	200	120	620.0 ± 8.0	-16.3 ± 0.7	3.3 ± 0.1	161.0 ± 20.2	629.0 ± 38.0	0.764 ± 0.002

Table 2. *p* values for the response surface model of CS_{CG}.

	μ	ζ	D_{10}	D_{50}	D_{90}	R
A: [Enzyme]	0.0001*	0.4350	0.7246	0.0000*	0.0007*	0.0027*
B: HT	0.0002*	0.7899	0.0000*	0.1641	0.8758	0.6633
AA	0.0000*	0.0180*	0.0582	0.0498*	0.3281	0.0006*
AB	0.0129*	0.6048	0.6053	0.1376	0.8491	0.7524
BB	0.7153	0.3964	0.0004*	0.0012*	0.7438	0.6908

*Statistical significance (*p* value < 0.05).

components leached from the particles and the original ones from the aqueous phase, it increases total solids and μ of CS_{CG}.

On the other hand, the hydrolysis of cellulose present in the skin and the seed shell acts on the crystalline part. In other words, it breaks the crystallinity of the cellulose fraction because of the endo-β glucanase action occurring in the enzymatic complex, generating amorphous polymers (celluoligosaccharides) with more significant interaction with water molecules through H_2 bonds. A greater number of OH groups exposed, restricting their mobility, and therefore, it contributes to the increased μ of CS_{CG} (Chami Khazraji & Robert, 2013).

Some authors have reported an opposite behavior in the μ of the filtered gooseberry juice when treated by enzymatic hydrolysis with Pectinex at different contents of total solids and [Enzyme] (Ramadan & Moersel, 2007). This has been attributed to the pectinases present, which decompose the pectic groups or polysaccharide substrates contained in the cell walls of the plant system.

The response surface graph 1A shows that the main effect of [Enzyme] and HT on the high μ of CS_{CG} occurs when they are at levels above 150 ppm and 60 minutes, respectively. This is potentiated by the positive HT-[Enzyme] interaction; that is to say, μ tends to be maximized (620 cP) at 200 ppm and 120 minutes. By increasing the [Enzyme], there are more enzyme molecules available to cleave the polysaccharide matrix of the cell wall, releasing more compounds present inside the cells (de Figueiredo et al., 2018)

In CS_{CG}, the value of ζ is a parameter of great importance related to its physicochemical stability and composition. It is mainly an indicator of the magnitude of the repulsive or electrostatic forces between adjacent colloidal particles (Yu et al., 2016). ζ presented significant statistical differences ($p < 0.05$) only with respect to the quadratic interaction of the [Enzyme] with mean values fluctuating between -16.2 and-20.8 mV. This identifies a layer of co-ions (Stern's layer) that is negatively charged and adsorbed at the interface of particles, mainly constituted by the insoluble material and the fatty component (Puente et al., 2011). On the other hand, the negative charge of the Stern layer is mainly composed of dissociated anions in the aqueous phase of CS_{CG} and by a non-hydrolyzed pectin coating that retains its negative charge (Cano-Sarmiento et al., 2018). In addition, the second electrical layer or positively charged and densely populated diffuse layer by the dissociated cations (Ca, P, Fe) of the aqueous phase make up the double electrical layer that allows stabilizing the adjacent particles due to the electrostatic repulsion between them (Fustier et al., 2010). However, CS_{CG} global stability is governed mainly by the balance of the repulsive and attractive forces (Van der Waals forces). The latter is directly related to the permanent or induced dipole interactions and the interactions of non-polar molecules, which are enhanced by the larger particle sizes (Genovese & Lozano, 2006). Other types of forces could be participating but to a lesser extent, and these include: steric, hydration, hydrophobic, and phase separation (Yu et al., 2016; Zhu et al., 2020).

The behavior of ζ in the response surface graph 1B shows a curvilinear trend, characteristic of the quadratic interaction. The greatest negative charge (<ζ) was in the vicinity of the Stern layer and is reached when CS_{CG} is enzymatically treated at [Enzyme] between 100 - 150 ppm. The observed behavior may be attributed to insoluble particles (fibers) when subjected to both enzymatic hydrolysis and shear stress, tend to decrease in size and, thus, increase the surface area and optical density (Zhou et al., 2017). Therefore, the enzymatic effect causes the chemical composition to vary (hydrolyzed polymers of lower molecular weight), and the interactions of H_2 bonds increase because of greater exposure of the glucose OH groups, which produces more excellent solubility and stability. If the size is smaller, it also reduces the gravitational effects and power CS_{CG} Brownian motion, reducing the possible precipitation of the particles. This phenomenon is evidenced by the increase in |ζ|, inferring that the electrostatically repulsive interactions increase when the number of species resulting from enzymatic hydrolysis increases (Yu et al., 2016).

The ζ results are comparable with the data reported by Zhu et al. (2020) for apple juice at different particle sizes (-12 to -16 mV), where the lowest values (> negative charge) are obtained at smaller particle sizes. On the other hand, Zhou et al. (2017) reported that mango juice presented mean values between −15.9 and −17.0 mV at high pressures. Wan et al. (2019) reported mean values between -19.0 and -20.5 mV for carrot juice fermented by probiotics. Some authors recommend that the limit of ζ in colloidal systems should be on |30| mV (Cano-Sarmiento et al., 2018). However, other researchers have reported physicochemically stable colloidal systems based on cape gooseberry, strawberry, and blackberry, due to the synergistic effect between μ and ζ (Gallón et al., 2020).

The D_{10} and D_{50} percentiles presented statistically significant differences (p <0.05) concerning the HT and [Enzyme] variables, respectively, in addition to the quadratic interactions of HT. The D_{90} percentile presented statistically significant differences (p <0.05), only concerning [Enzyme]. The mean values of D_{10}, D_{50},

and D_{90} fluctuated between (2.4 - 12.7 µm), (104.1 - 142.3 µm), and (449.3 - 649.3 µm), respectively. This denotes a lower effect of the D_{10} enzymatic treatments (< degree of variability), followed by D_{50} and D_{90}, and the latter condition was the most representative or critical. Consequently, the cumulative 10% corresponds to individual cells and/or cell fragments; whereas, D_{50} values> 100 µm can be small groups of cells or tissue fragments that grow due to the attractive forces of these particles, which finally up in larger groups that represent the D_{90} values.

According to the response surface graphs, the behavior shows that D_{10} (Figure 1C) decreases with the increase in HT; however, these changes were not considered critical since these particles are coupled within CS_{CG} particle Brownian motion. On the other hand, the D_{50} percentile (Figure 1D) showed a tendency to decrease with low [Enzyme], presenting the lowest values under HT conditions (45 - 75 minutes) and [Enzyme] (50 - 75 ppm). In addition, the effect of the HT quadratic interaction was observed, presenting a curvilinear behavior, which causes the curvature minima to increase with the increase of [Enzyme]. For the case of D_{90} (Figure 1E), a directly proportional relationship was observed between the HT and [Enzyme], which favors the lowest D_{90} values when the [Enzyme] was <125 ppm. In general,

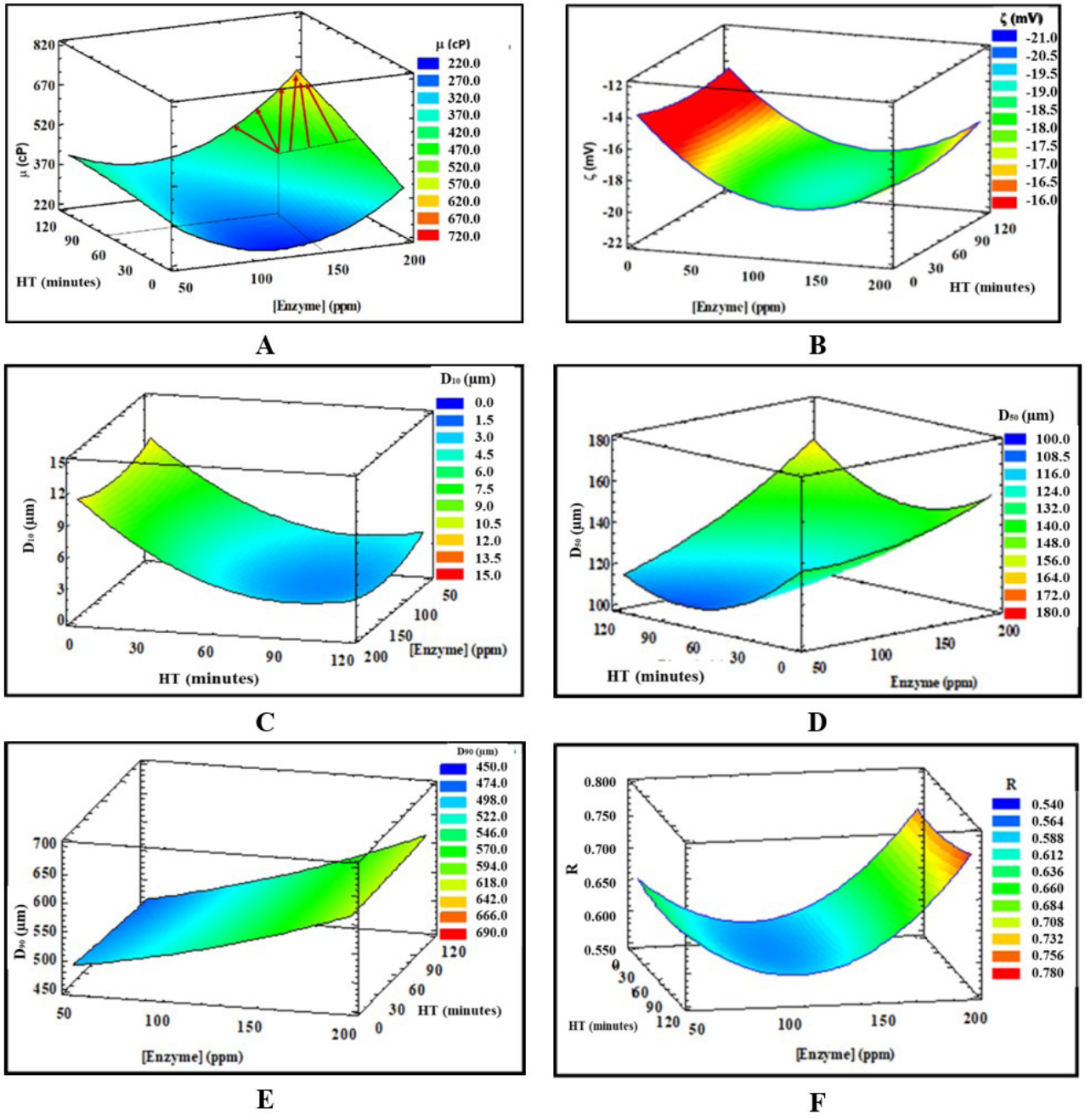

Figure 1. Response surfaces of the dependent variables as a function of the independent variables of CS_{CG}. (A) Viscosity; (B) Zeta Potential; (C) Particle Size D_{10}; (D) Particle Size $D_{50;}$ (E) Particle Size D_{90}. (F) Spectral absorption index (R).

D_{50} and D_{90} behaved similarly, and this could be attributed to the resulting main phenomena: 1) weakening of the insoluble structure caused during the enzymatic hydrolysis process (Álvarez García, 2018), which confers a decrease in particle sizes; 2) saturation of enzymes on particle surfaces when the formulation contains high [Enzyme]. This second effect inhibited enzyme action without effectively reducing particle sizes and favoring attractive forces, which could confer aggregates and/or phase separations in CS_{CG} (Carlos et al., 2018).

Dahdouh et al. (2018) stated that juices could be considered polydisperse suspensions that appear based on the predominant particle size. Thus, these colloidal systems can fit between those particle sizes <1 μm, the supracolloidal systems between 1 μm and 100 μm, and those whose particles are much larger (> 100 μm), where gravitational effects become more evident and physicochemical instability is more frequent. In general, most research evaluates the effect of high shear homogenization pressures on the particle size of juices or suspensions of plant structures such as cashew (Leite et al., 2015), pineapple (Silva et al., 2010), sugar beet (Huang et al., 2020), and tomato (Augusto et al., 2012), among others, and they concluded that higher pressures or homogenization times result in reduced particle size. Various investigations evaluate the effect of enzymatic hydrolysis in fruit juices or suspensions. However, the objectives are principally oriented to evaluate the influence on turbidity, rheology, disposition and extraction of bioactive compounds, clarification, and yield (Borchani et al., 2019; Cerreti et al., 2016; Chang et al., 2018; Gouvêa et al., 2017; Handique et al., 2019; Machado et al., 2016; Maktouf et al., 2014; Phuong & Tuan, 2016). It is considered that the integration of shear homogenization processes with enzymatic treatments generates greater synergy in size reduction; however, the literature does not report studies in this regard.

The R is an indirect indicator of the stability of the particles in CS_{SG}, which relates the particle size distributions with the light scattering at different wavelengths. Furthermore, the scattering of light in a colloidal system increases as the particle size decreases, and the light wavelength shortening results in the more significant scattering of light (Kaufman & Garti, 1981). The absorbance ratio at 400 and 800 nm (R = A800 / A400) has been associated with the level of light absorption in colloidal systems and is related to their stability. It is more stable when R is lower because of the higher number of smaller particles, which absorb more light (Horie et al., 1976).

The R presented statistically significant differences ($p < 0.05$) concerning [Enzyme]. Moreover, its quadratic interaction was reflected in the high fluctuations observed in its mean values (0.540 - 0.784). This allows for determining the main effect of larger sizes and more considerable variations of D_{50} (104.1-142.3 μm) and D_{90} (449.3 - 649.3 μm), which causes them to absorb less incident light (Mirhosseini et al., 2008). This is corroborated by the response surface graph (Figure 1F), which shows more similar R behaviors between D_{50} and D_{90}. A trend of higher R values is noted when CS_{CG} operates at higher [Enzyme] (150-200 ppm). This is related to the larger size of the dispersed material in CS_{CG} (skin and seed of the gooseberry that does not achieve effective hydrolysis by the enzyme complex); however, the quadratic interaction enhances low R values for [Enzyme] between 100 and 125 ppm. In all cases, an influence of HT is not observed, and this study is highlighted as the first that evaluates the enzymatic effect on R.

3.2 Mathematical modeling and experimental optimization of multiple responses.

Table 3 presents the estimated regression coefficients of the 2nd order polynomial model for CS_{CG} and their respective R^2. The R^2 values for the dependent variables μ, D_{10}, D_{50}, D_{90}, and R showed a good fit for the mathematical model; whereas, the adjustment for the rest of the variables is considered acceptable. This is because the conditions imposed during mixing in the HT could have affected these variables, making the error concerning the value predicted by the model more excellent. A random distribution of the residuals was observed in all the variables, making it possible to ensure that the data can be parameterized according to a normal distribution. Therefore, the models are adequate to describe the behavior of the observed results.

Furthermore, it presents the theoretical results obtained by the 2nd order polynomial models and the experimental results obtained at the determined optimal condition. Table 4 presents the criteria, weights, and impacts of the dependent variables considered for the experimental optimization of a physiochemically stable CS_{CG} and considering the ANOVA results. In addition, the theoretical values predicted by the mathematical model are presented; as well as the experimental values validated from 3 replicates in the optimal condition obtained and the relative mean error RME = |(theoretical-experimental)/theoretical) *100|. The results obtained from the optimization defined the dependent variables: [Enzyme] = 78.5 ppm and HT = 120 min, with a desirability of 74.2%. RME values were less than 20% in all cases; therefore, it is considered that the multiple response optimization models present an acceptable level of prediction

Table 3. Polynomial regression coefficients and R^2 for the surface model of $CS_{CG.}$

Coefficients	μ (cP)	ζ (mV)	D_{10} (μm)	D_{50} (μm)	D_{90} (μm)	R
β_0	618.8	-13.6	13.5	141.0	480.8	0.8
β_A	-6.6	-0.1	-0.05	-0.2	0.2	-0.0045
β_B	0.2	-0.03	-0.2	-0.9	-0.4	-0.0004
β_{AB}	0.01	0.0001	0.0001	0.0012	0.0008	-
β_A^2	0.03	0.0004	0.0002	0.0002	0.0042	-
β_B^2	-0.002	0.0003	0.0010	0.0055	0.0024	-
R^2	**95.0**	**53.0**	**93.8**	**90.5**	**74.9**	**83.1**

Table 4. Comparison of model prediction results against experimental values under optimal conditions.

Variable	Criterion	Impact	Weight	Predicted value	Experimental value	RME (%)
μ(cP)	Maximize	0.8	4.0	356.9	371.3 ± 24.4	4.0
ζ (mV)	Minimize	0.8	4.0	-18.5	-21.8 ± 0.3	18.0
D_{10} (μm)	Minimize	0.5	3.0	3.2	3.5 ± 0.3	9.4
D_{50} (μm)	Minimize	0.8	4.0	118.3	135 ± 3.6	14.2
D_{90} (μm)	Minimize	1.0	5.0	480.8	565.7 ± 25.5	17.6
R	Minimize	0.8	4.0	0.605	0.655 ± 0.007	8.2

for the experimental data. In their work, Handique et al. (2019) optimized banana juice based on the desirability, obtaining a value of 74.25%, similar to this study.

4 Conclusions

The present research allowed for the development of a sustainable process that integrated shearing homogenization with enzymatic treatments. Cape gooseberry pulp, skin, and seed were used to obtain a colloidal system, which can be used in various agro-industrial processes. In the enzymatic hydrolysis process, the independent variable [Enzyme] mainly influenced the dependent variables μ, D_{50}, $D_{90,}$ and R; while the HT influenced the μ, SS, and D_{10}. Furthermore, the [Enzyme] - HT interaction affects the increase in μ. The enzymatic hydrolysis process conferred a decrease in the size of the particles (minors attractive forces) in the CS_{CG}; therefore, the physicochemical stability was improved compared to CS_{CG} without enzymatic treatment (D_{10}: 16.8 μm, D_{50}: 166 μm and D_{90}: 660 μm). However, the low values of μ (371.3 cP) and ζ (-21.8 mV) and high values of particle size (D_{10}: 3.5 μm, D_{50}: 135 μm, and D_{90}: 565.7 μm), and R (0.655) do not guarantee that the CS_{CG} will have good long-term stability. Therefore, it is recommended that 1) monovalent ions (Na^{+1} and Cl^{-1}) be added to increase the ionic strength and the width of the electric double layer to increase the repulsive forces of the colloidal system; 2) a hydrocolloid be added to increase the viscosity of the continuous phase and decrease the mobility of the particles; and 3) achieve greater disintegration of the particles, using high-pressure homogenization systems, which would reduce the attractive or Van der Waals forces.

Conflict of interest

The authors have declared no conflicts of interest for this article.

Acknowledgements

The authors are grateful to Ministerio de Ciencia, Tecnología e Innovación, Sistema General de Regalías del Departamento de Antioquia, Proexcar, Universidad Nacional de Colombia campus Medellín and Gobernación del departamento de Nariño.

References

Agarwal, R., & Bosco, S. (2014). Optimization of Viscozyme-L assisted extraction of coconut milk and virgin coconut oil. *Asian Journal of Dairy and Food Research*, 33(4), 276-284. http://dx.doi.org/10.5958/0976-0563.2014.00617.4.

Álvarez García, C. (2018). Application of enzymes for fruit juice processing. In G. Rajauria & B. Tiwari (Eds.), *Fruit juices: extraction, composition, quality and analysis* (pp. 201-216). Cambridge: Academic Press. http://dx.doi.org/10.1016/B978-0-12-802230-6.00011-4.

Areiza-Mazo, N., Robles, J., Zamudio-Rodriguez, J. A., Giraldez, L., Echeverria, V., Barrera-Bailon, B., Aliev, G., Sahebkar, A., Ashraf, G. M., & Barreto, G. E. (2018). Extracts of Physalis peruviana protect astrocytic cells under oxidative stress with rotenone. *Frontiers in Chemistry*, 6(276), 1-13. http://dx.doi.org/10.3389/fchem.2018.00276. PMid:30175092.

Association of Official Analytical Chemists – AOAC. (2012). *Official methods of analysis of the Association of Official Analytical Chemists* (19th ed.). Arlington: AOAC.

Augusto, P., Ibarz, A., & Cristianini, M. (2012). Effect of high pressure homogenization (HPH) on the rheological properties of tomato juice: time-dependent and steady-state shear. *Journal of Food Engineering*, 111(4), 570-579. http://dx.doi.org/10.1016/j.jfoodeng.2012.03.015.

Borchani, M., Masmoudi, M., Ben Amira, A., Abbès, F., Yaich, H., Besbes, S., Blecker, C., Garvin, A., Ibarz, A., & Attia, H. (2019). Effect of enzymatic treatment and concentration method on chemical, rheological, microstructure and thermal properties of prickly pear syrup. *Lebensmittel-Wissenschaft + Technologie*, 113, 108314. http://dx.doi.org/10.1016/j.lwt.2019.108314.

Cano-Sarmiento, C., Téllez-Medina, D. I., Viveros-Contreras, R., Cornejo-Mazón, M., Figueroa-Hernández, C. Y., García-Armenta, E., Alamilla-Beltrán, L., García, H. S., & Gutiérrez-López, G. F. (2018). Zeta Potential of Food Matrices. *Food Engineering Reviews*, 10(3), 113-138. http://dx.doi.org/10.1007/s12393-018-9176-z.

Carlos, L. A. J., Cynthia, T. C., & Misael, C. R. (2018). Influence of the composition of coconut-based emulsions on the stability of the colloidal system. *Advance Journal of Food Science and Technology*, 14(3), 77-92. http://dx.doi.org/10.19026/ajfst.14.5841.

Cerreti, M., Liburdi, K., Benucci, I., & Esti, M. (2016). The effect of pectinase and protease treatment on turbidity and on haze active molecules in pomegranate juice. *Lebensmittel-Wissenschaft + Technologie*, 73, 326-333. http://dx.doi.org/10.1016/j.lwt.2016.06.030.

Chami Khazraji, A., & Robert, S. (2013). Interaction effects between cellulose and water in nanocrystalline and amorphous regions: a novel approach using molecular modeling. *Journal of Nanomaterials*, 2013, 1-10. http://dx.doi.org/10.1155/2013/409676.

Chang, L. S., Karim, R., Sabo Mohammed, A., & Mohd Ghazali, H. (2018). Characterization of enzyme-liquefied soursop (Annona muricata L.) puree. *Lebensmittel-Wissenschaft + Technologie*, 94, 40-49. http://dx.doi.org/10.1016/j.lwt.2018.04.027.

Chen, J., Wu, S.-S., Liang, R.-H., Liu, W., Liu, C.-M., Shuai, X.-X., & Wang, Z.-J. (2014). The effect of high speed shearing on disaggregation and degradation of pectin from creeping fig seeds. *Food Chemistry*, 165, 1-8. http://dx.doi.org/10.1016/j.foodchem.2014.05.096. PMid:25038641.

Dahdouh, L., Delalonde, M., Ricci, J., Ruiz, E., & Wisnewski, C. (2018). Influence of high shear rate on particles size, rheological behavior and fouling propensity of fruit juices during crossflow microfiltration: Case of orange juice. *Innovative Food Science & Emerging Technologies*, 48, 304-312. http://dx.doi.org/10.1016/j.ifset.2018.07.006.

Dahdouh, L., Wisniewski, C., Ricci, J., Vachoud, L., Dornier, M., & Delalonde, M. (2016). Rheological study of orange juices for a better knowledge of their suspended solids interactions at low and high concentration. *Journal of Food Engineering*, 174, 15-20. http://dx.doi.org/10.1016/j.jfoodeng.2015.11.008.

de Figueiredo, V. R. G., Yamashita, F., Vanzela, A. L. L., Ida, E. I., & Kurozawa, L. E. (2018). Action of multi-enzyme complex on protein extraction to obtain a protein concentrate from okara. *Journal of Food Science and Technology*, 55(4), 1508-1517. http://dx.doi.org/10.1007/s13197-018-3067-4. PMid:29606765.

Fuente, F. P., Nocetti, D., Sacristán, C., Ruiz, P., Guerrero, J., Jorquera, G., Uribe, E., Bucarey, J. L., Espinosa, A., & Puente, L. (2020). *Physalis peruviana* L. Pulp prevents liver inflammation and insulin resistance in skeletal muscles of diet-induced obese mice. *Nutrients*, 12(3), 700. http://dx.doi.org/10.3390/nu12030700. PMid:32151028.

Fustier, P., Taherian, A. R., & Ramaswamy, H. S. (2010). Emulsion delivery systems for functional foods. In J. Smith & E. Charter (Eds.), *Functional food product development* (pp. 79-97). Hoboken: Blackwell Publishing Ltd. http://dx.doi.org/10.1002/9781444323351.ch4

Gallón, M., Cortés, M., & Gil, J. (2020). Physicochemical stability of colloidal systems using the cape gooseberry, strawberry, and blackberry for spray drying. *Journal of Food Processing and Preservation*, 44(9), 1-10. http://dx.doi.org/10.1111/jfpp.14705.

Genovese, D., & Lozano, J. (2006). Contribution of colloidal forces to the viscosity and stability of cloudy apple juice. *Food Hydrocolloids*, 20(20), 767-773. http://dx.doi.org/10.1016/j.foodhyd.2005.07.003.

Gouvêa, R. F., Ribeiro, L. O., Souza, É. F., Penha, E. M., Matta, V. M., & Freitas, S. P. (2017). Effect of enzymatic treatment on the rheological behavior and vitamin C content of Spondias tuberosa (umbu) pulp. *Journal of Food Science and Technology*, 54(7), 2176-2180. http://dx.doi.org/10.1007/s13197-017-2630-8. PMid:28720976.

Handique, J., Bora, S., & Sit, N. (2019). Optimization of banana juice extraction using combination of enzymes. *Journal of Food Science and Technology*, 56(8), 3732-3743. http://dx.doi.org/10.1007/s13197-019-03845-z. PMid:31413400.

Hennart, S., Wildeboer, W., van Hee, P., & Meesters, G. (2010). Stability of particle suspensions after fine grinding. *Powder Technology*, 199(3), 226-231. http://dx.doi.org/10.1016/j.powtec.2010.01.010.

Horie, K., Tanaka, S., & Akabori, T. (1976). Determination of emulsion stability by spectal absorption; Part 1. *Journal of Society of Cosmetic Chemists of Japan*, 10(1-2), 28-33. http://dx.doi.org/10.5107/sccj1976.10.28.

Hua, X., Xu, S., Wang, M., Chen, Y., Yang, H., & Yang, R. (2017). Effects of high-speed homogenization and high-pressure homogenization on structure of tomato residue fibers. *Food Chemistry*, 232, 443-449. http://dx.doi.org/10.1016/j.foodchem.2017.04.003. PMid:28490096.

Huang, X., Liu, Q., Yang, Y., & He, W. (2020). Effect of high pressure homogenization on sugar beet pulp: rheological and microstructural properties. *Lebensmittel-Wissenschaft + Technologie*, 125, 2-8. http://dx.doi.org/10.1016/j.lwt.2020.109245.

Instituto Colombiano de Normas Técnicas y Certificación – ICONTEC. (1999). *Fresh fruits. Cape gooseberry. Specifications* (NTC 4580:1999, pp. 17). Bogotá: ICONTEC.

Kaufman, V., & Garti, N. (1981). Spectral absorption measurements for determination of ease of formation and stability of oil in water emulsions. *Journal of Dispersion Science and Technology*, 2(4), 475-490. http://dx.doi.org/10.1080/01932698108943925.

Kitrytė, V., Kraujalienė, V., Šulniūtė, V., Pukalskas, A., & Venskutonis, P. (2017). Chokeberry pomace valorization into food ingredients by enzyme-assisted extraction: Process optimization and product characterization. *Food and Bioproducts Processing*, 105, 36-50. http://dx.doi.org/10.1016/j.fbp.2017.06.001.

Leite, T., Augusto, P., & Cristianini, M. (2015). Using High Pressure Homogenization (HPH) to Change the Physical Properties of Cashew Apple Juice. *Food Biophysics*, 10(2), 169-180. http://dx.doi.org/10.1007/s11483-014-9385-9.

López-Esparza, R., Balderas Altamirano, M. A., Pérez, E., & Gama Goicochea, A. (2015). Importance of molecular interactions in colloidal dispersions. *Advances in Condensed Matter Physics*, 2015, 1-8. http://dx.doi.org/10.1155/2015/683716.

Machado, B., Costa, A., Oliveira, R., Barreto, G., Silva, R., & Umsza, M. (2016). Effect of applying pectinolytic enzymes in Spondias tuberosa Arr. Cam. Pulp. *Revista Virtual de Quimica*, 8(4), 1067-1078. http://dx.doi.org/10.21577/1984-6835.20160076.

Maktouf, S., Neifar, M., Drira, S. J., Baklouti, S., Fendri, M., & Châabouni, S. E. (2014). Lemon juice clarification using fungal pectinolytic enzymes coupled to membrane ultrafilt. *Food and Bioproducts Processing*, 92(1), 14-19. http://dx.doi.org/10.1016/j.fbp.2013.07.003.

Matusiak, J., & Grządka, E. (2017). Stability of colloidal systems - a review of the stability measurements methods. *Annales Universitatis Mariae Curie-Sklodowska. Sectio AA, Chemia*, 72(1), 33. http://dx.doi.org/10.17951/aa.2017.72.1.33.

Mirhosseini, H., Tan, C., Hamid, N., & Yusof, S. (2008). Effect of Arabic gum, xanthan gum and orange oil contents on ζ-potential, conductivity, stability, size index and pH of orange beverage emulsion. *Colloids and Surfaces. A, Physicochemical and Engineering Aspects*, 315(1-3), 47-56. http://dx.doi.org/10.1016/j.colsurfa.2007.07.007.

Mokhtar, S. M., Swailam, H. M., & Embaby, H. E. S. (2018). Physicochemical properties, nutritional value and techno-functional properties of goldenberry (Physalis peruviana) waste powder concise title: composition of goldenberry juice waste. *Food Chemistry*, 248, 1-7. http://dx.doi.org/10.1016/j.foodchem.2017.11.117. PMid:29329831.

Nocetti, D., Núñez, H., Puente, L., Espinosa, A., & Romero, F. (2020). Composition and biological effects of goldenberry byproducts: an overview. *Journal of the Science of Food and Agriculture*, 100(12), 4335-4346. http://dx.doi.org/10.1002/jsfa.10386. PMid:32198760.

Olivares, M., Dekker, M., Verkerk, R., & van Boekel, M. (2016). Health-promoting compounds in cape gooseberry (Physalis peruviana L.): review from a supply chain perspective. *Trends in Food Science and Technology*, 57(Pt A), 83-92. https://doi.org/10.1016/j.tifs.2016.09.009.

Ozyurt, V. H., & Ötles, S. (2016). Effect of food processing on the physicochemical properties of dietary fibre. *Acta Scientiarum Polonorum. Technologia Alimentaria*, 15(3), 233-245. http://dx.doi.org/10.17306/J.AFS.2016.3.23. PMid:28071023.

Phuong, N., & Tuan, Q. (2016). Application of hydrolytic enzymes for improvement of red dragon fruit juice processing. *Asia Pacific Journal of Sustainable Agriculture Food and Energy*, 4(1), 1-4.

Puente, L. A., Pinto-Muñoz, C. A., Castro, E. S., & Cortés, M. (2011). Physalis peruviana Linnaeus, the multiple properties of a highly functional fruit: a review. *Food Research International*, 44(7), 1733-1740. http://dx.doi.org/10.1016/j.foodres.2010.09.034.

Ramadan, M. (2011a). Physalis peruviana: a rich source of bioactive phytochemicals for functional foods and pharmaceuticals. *Food Reviews International*, 27(3), 259-273. http://dx.doi.org/10.1080/87559129.2011.563391.

Ramadan, M. (2011b). Bioactive phytochemicals, nutritional value, and functional properties of cape gooseberry (Physalis peruviana): An overview. *Food Research International*, 44(7), 1830-1836. http://dx.doi.org/10.1016/j.foodres.2010.12.042.

Ramadan, M. (2018). Enzymes in fruit juice processing. In M. Kuddus (Ed.), *Enzymes in food biotechnology: production, applications, and future prospects* (pp. 45-59). USA: Elsevier. https://doi.org/10.1016/B978-0-12-813280-7.00004-9

Ramadan, M., & Moersel, J. (2007). Impact of enzymatic treatment on chemical composition, physicochemical properties and radical scavenging activity of goldenberry (Physalis peruviana L.) juice. *Journal of the Science of Food and Agriculture*, 87(3), 452-460. http://dx.doi.org/10.1002/jsfa.2728.

Ramadan, M., & Morsel, J. (2003). Oil goldenberry (Physalis peruviana L.). *Journal of Agricultural and Food Chemistry*, 51(4), 969-974. http://dx.doi.org/10.1021/jf020778z. PMid:12568557.

Ramadan, M., Sitohy, M., & Moersel, J. (2008). Solvent and enzyme-aided aqueous extraction of goldenberry (*Physalis peruviana* L.) pomace oil: Impact of processing on composition and quality of oil and meal. *European Food Research and Technology*, 226(6), 1445-1458. http://dx.doi.org/10.1007/s00217-007-0676-y.

Silva, V. M., Sato, A. C. K., Barbosa, G., Dacanal, G., Ciro-Velásquez, H. J., & Cunha, R. L. (2010). The effect of homogenisation on the stability of pineapple pulp. *International Journal of Food Science & Technology*, 45(10), 2127-2133. http://dx.doi.org/10.1111/j.1365-2621.2010.02386.x.

Singh, J., Kundu, D., Das, M., & Banerjee, R. (2019). Enzymatic processing of juice from fruits/vegetables: An emerging trend and cutting edge research in food biotechnology. In M. Kuddus (Ed.), *Enzymes in food biotechnology: production, applications, and future prospects* (pp. 419-432). USA: Elsevier Inc. http://dx.doi.org/10.1016/B978-0-12-813280-7.00024-4

Uzuner, S., & Cekmecelioglu, D. (2018). Enzymes in the beverage industry. In M. Kuddus (Ed.), *Enzymes in food biotechnology: production, applications, and future prospects* (pp. 29-43). USA: Elsevier Inc. https://doi.org/10.1016/B978-0-12-813280-7.00003-7

Vijayanand, P., Kulkarni, S., & Prathibha, G. (2010). Effect of pectinase treatment and concentration of litchi juice on quality characteristics of litchi juice. *Journal of Food Science and Technology*, 47(2), 235-239. http://dx.doi.org/10.1007/s13197-010-0023-3. PMid:23572631.

Vong, W., & Liu, S. (2019). The effects of carbohydrase, probiotic Lactobacillus paracasei and yeast Lindnera saturnus on the composition of a novel okara (soybean residue) functional beverage. *Lebensmittel-Wissenschaft + Technologie*, 100, 196-204. http://dx.doi.org/10.1016/j.lwt.2018.10.059.

Wan, Y., Xu, M., Gilbert, R., Yin, J., Huang, X., Xiong, T., & Xie, M. (2019). Colloid chemistry approach to understand the storage stability of fermented carrot juice. *Food Hydrocolloids*, 89, 623-630. http://dx.doi.org/10.1016/j.foodhyd.2018.11.017.

Wardy, W., Pujols Martínez, K. D., Xu, Z., No, H. K., & Prinyawiwatkul, W. (2014). Viscosity changes of chitosan solution affect physico-functional properties and consumer perception of coated eggs during storage. *Lebensmittel-Wissenschaft + Technologie*, 55(1), 67-73. http://dx.doi.org/10.1016/j.lwt.2013.07.013.

Wellala, C., Bi, J., Liu, X., Liu, J., Lyu, J., Zhou, M., Marszałek, K., & Trych, U. (2020). Effect of high pressure homogenization combined with juice ratio on water-soluble pectin characteristics, functional properties and bioactive compounds in mixed juices. *Innovative Food Science & Emerging Technologies*, 60(2), 102279. http://dx.doi.org/10.1016/j.ifset.2019.102279.

Yu, Z., Jiang, S., Cao, X., Jiang, S., & Pan, L. (2016). Effect of high pressure homogenization (HPH) on the physical properties of taro (*Colocasia esculenta* (L). Schott) pulp. *Journal of Food Engineering*, 177, 1-8. http://dx.doi.org/10.1016/j.jfoodeng.2015.10.042.

Zhou, L., Guan, Y., Bi, J., Liu, X., Yi, J., Chen, Q., Wu, X., & Zhou, M. (2017). Change of the rheological properties of mango juice by high pressure homogenization. *Lebensmittel-Wissenschaft + Technologie*, 82, 121-130. http://dx.doi.org/10.1016/j.lwt.2017.04.038.

Zhu, D., Shen, Y., Wei, L., Xu, L., Cao, X., Liu, H., & Li, J. (2020). Effect of particle size on the stability and flavor of cloudy apple juice. *Food Chemistry*, 328, 126967. http://dx.doi.org/10.1016/j.foodchem.2020.126967. PMid:32505057.